Advanced Composite Materials
Publication details, including instructions for authors and subscription information:
http://www.tandfonline.com/loi/tacm20

Postbuckled behavior of composite isogrid stiffened shell structure

Thomas D. Kim

Version of record first published: 02 Apr 2012.

To cite this article: Thomas D. Kim (2000): Postbuckled behavior of composite isogrid stiffened shell structure, Advanced Composite Materials, 9:3, 253-263

To link to this article: http://dx.doi.org/10.1163/15685510051033467

Adv. Composite Mater., Vol. 9, No. 3, pp. 253–263 (2000)

Postbuckled behavior of composite isogrid stiffened shell structure

THOMAS D. KIM

Asian Office of Aerospace Research and Development, 7-23-17 Roppongi, Minato-ku, Tokyo, Japan
E-mail: kimt@aoard.af.mil

Received 17 January 2000; accepted 17 April 2000

Abstract—This paper investigated reliability of a postbuckled composite isogrid stiffened shell structure under a compression load. The outside diameter of the isogrid cylinder was 624.8 mm, the length was 368.3 mm and the total weight of the cylinder was 3.24 kg. A finite element buckling analysis result was compared with the axial compression experimental data. The average critical buckling load of 186.56 kN was obtained by using the Patran finite element analysis (FEA). The isogrid shell was modeled using 3-node triangular elements and the stiffeners were modeled using 4-node quad elements with a total of 504 nodes and 900 elements. The postbuckled isogrid cylinder was compression tested to the failure load of 177.35 kN. The postbuckled cylinder continued to resist compression loading even after one or more stiffeners had fractured. The testing evaluation revealed that the stiffener buckling was the critical failure mode and it has been demonstrated to be tolerant to structural damage due to the multiplicity of load paths. The lower experimental bucking load was due to the small imperfections in the cylinder but this problem can be overcome by advancement in the manufacturing methods.

Keywords: Composite; isogrid; stiffened; buckling; cylinder; manufacturing; compression.

1. INTRODUCTION

The development of lightweight and highly efficient structural components is desirable for the next generation of aerospace systems [1]. The use of composite materials for space application is particularly attractive because space structures are stiffness driven and require stringent weight limits. The combination of composite materials and an isogrid stiffened design is particularly well suited for critical structures that require buckling resistance and damage tolerance [2]. When the structure is stiffened, it typically means that a ring or oddly shaped pieces of metal are added to the backside of a plate or shell, as shown in Fig. 1. This stiffening concept increases the buckling resistance and thus the critical loads can be delayed with only a little addition of material. The high performance launch vehicle

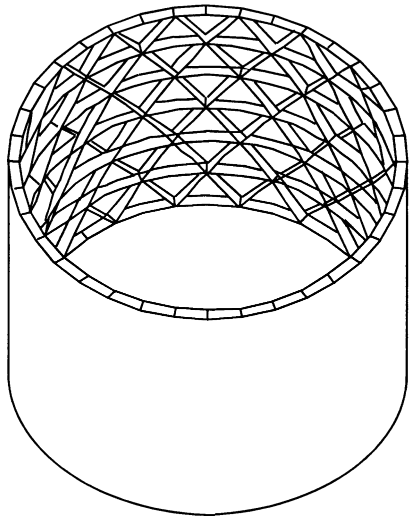

Figure 1. Isogrid stiffened cylinder.

structures, such as interstage and fairings, utilize metallic isogrid designs to transmit and sustain the applied loads. These current stiffened structures are machined from a single solid piece of metal to form the thin skin with stiffeners. This manufacturing process is costly and time consuming, requiring more than one year to fabricate a single large cylindrical stiffened structure. The introduction of composite isogrid structures into industry has so far been hampered by lack of understanding of isogrid failure behavior and manufacturing methods. This paper examined the postbuckling characteristics of a composite isogrid under the compressive load. Knowledge of the stability behavior is essential for construction of a reliable lightweight aerospace structure and will allow designers to add additional capabilities while reducing life cycle costs.

2. FABRICATION METHOD

The isogrid cylinder was fabricated from a carbon fiber reinforced epoxy in the form of a prepreg tow and unidirectional tape. The Hercules IM7 fiber and the toughened epoxy (977-2) resin system from Fiberite were used. The properties of IM7/977-2 are shown in Fig. 2. The manufacturing of isogrid structures has proven to be complex due to buildups at the stiffener node intersections where the fibers cross over [3]. At each intersection, three times the amount of fiber will cross over, making out-of-plane compaction difficult. Excessive buildup, if not designed and fabricated properly, will cause higher loads to be concentrated at the intersections (nodes). These non-uniformly distributed loads at the nodal points can cause a premature failure of the structure. One way to reduce the buildup is by offsetting the fibers at the nodal intersections. This offsetting allows each ply to overlap another by reducing from three plies to two plies [4].

Cylinder Outside Radius, (mm)	312.42
Cylinder Length, (mm)	368.30
0° Tensile Strength, (GPa)	2.82
0° Tensile Modulus, (GPa)	173
90° Tensile Strength, (MPa)	75.1
90° Tensile Modulus, (GPa)	7.60
0° Compression Modulus, (GPa)	157
Shear Modulus, (GPa)	5.50
0° Flexural Strength, (GPa)	1.64

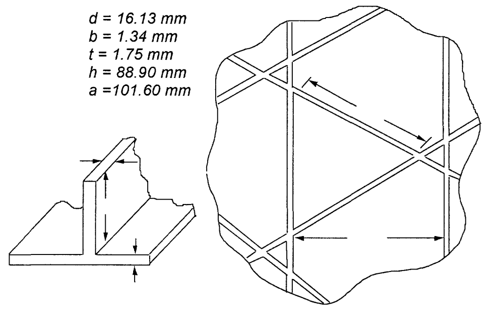

Figure 2. Isogrid dimensions.

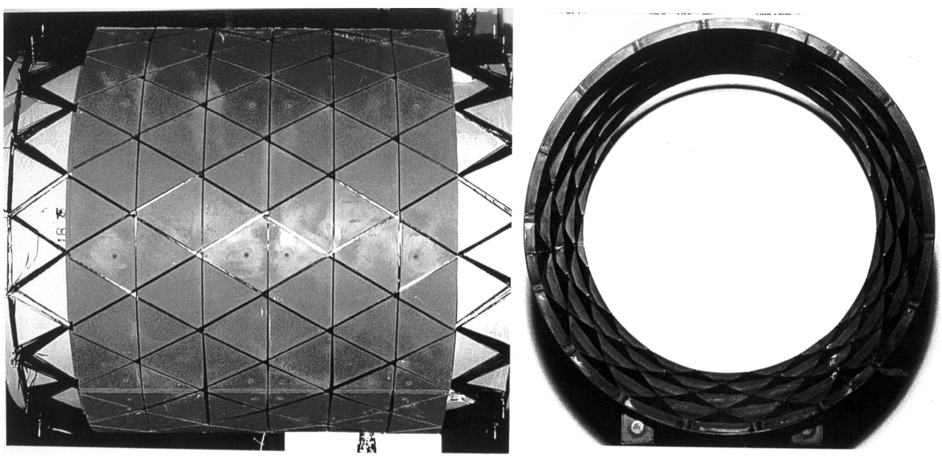

Figure 3. Isogrid cylinder fabrication.

Winding prepreg tow into isogrid shaped grooves (slots) formed the stiffeners in the rubber mold as shown in Fig. 3. The use of rubber tooling is critical because the rubber is primarily responsible for lateral compaction of the stiffeners. Between 40 to 50 layups are needed to fill the 1.45 cm deep slots by stacking each tow fiber on top of another until it was filled to the top. Then the skin was filament wound: it consisted of 12 plies of $[+90, 0, 90, 0]_s$ orientations. The entire part was bagged and co-cured in an autoclave. This procedure results in excellent stiffener consolidation and skin finish. After curing, the rubber mold is removed leaving a cylindrical composite isogrid as shown in Fig. 3. All curing was done in an autoclave for 2 h at 177°C and a pressure of 0.552 MPa.

3. FINITE ELEMENT ANALYSIS

The objective of the finite element analysis was to visualize the behavior of the isogrid cylinder under the compressive load and determine the maximum buckling strength. Five different linear finite element buckling analyses were

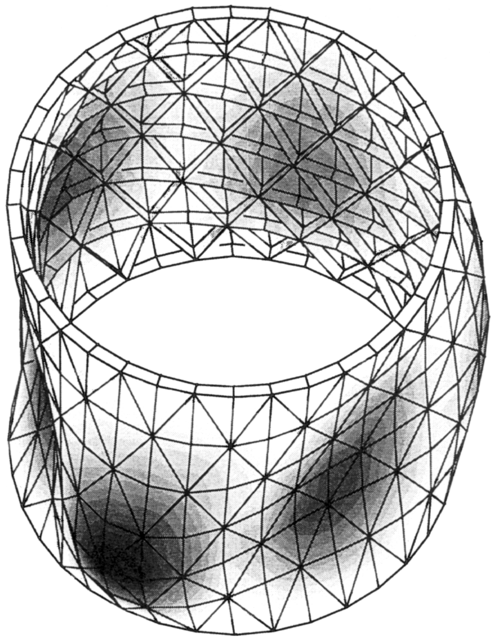

Figure 4. Buckled shape of cylinder.

performed using the parameters listed in Fig. 2. The cylinder model was analyzed using Patran pre- and post-processors. The geometry of the isogrid cylinder was generated by measuring various dimensions on the test specimen and averaging the results. The Patran model of the isogrid cylinder consists of 504 nodes and 900 elements. The isogrid skin was modeled using the 3-node triangular elements and the stiffeners were modeled using the 4-node quadrilateral elements. The boundary conditions were modeled as simply supported at both ends to simulate the actual test conditions. The deformed shapes of the isogrid cylinder under the axial compression load are shown in Fig. 4. The dark regions represent the stress concentrations around the cylinder where failure might occur. The effect of the stiffener/skin interface was difficult to determine from this analysis. The FEA

Table 1.
Finite element analysis results

Patran FEA model #	Stiffener thick (mm)	Stiffener height (mm)	Skin thick (mm)	Buckling load (kN)	Longitudinal disp. at buckling load (mm)
1	1.36	15.77	1.78	189.50	12.24
2	1.31	16.20	1.74	182.38	12.78
3	1.37	16.07	1.76	189.49	12.14
4	1.33	15.70	1.72	184.60	12.61
5	1.34	16.16	1.76	186.83	12.73

results are summarized in Table 1. The maximum load ranged from 189.5 kN to 182.4 kN with maximum displacement of 12.73 mm. The results indicate that for an isogrid cylinder, the skin thickness parameter had more influence in obtaining higher buckling load. However, the increase in skin thickness will increase weight, which will make the structure less efficient. It was expected to obtain lower buckling load from the experiment due to the fact that the cylinder was slightly damaged from the previous test and also the FEA did not consider minor manufacturing imperfections in the isogrid cylinder.

4. AXIAL COMPRESSION TEST

Shell stiffened structures are susceptible to failure by buckling and extensive research has been reported in the open literature [5, 6]. The objective of the compression test on the cylindrical composite isogrid structure was to examine the pre- and post-buckling characteristics and to determine the maximum load before the failure [7]. The outside diameter of isogrid cylinder was 624.8 mm, the length was 368.3 mm and the total weight of the cylinder was 3.24 kg. The top and bottom of the cylinder were potted with fiberglass and machined flat in order to evenly transmit the applied loads. The test fixture as shown in Fig. 5 was fabricated with precision ground 3.81 cm thick stainless steel top and base plates in which the cylinder was placed between the plates. The corners of the bottom plate had support pins that secured the cylinder during the compression test. The isogrid

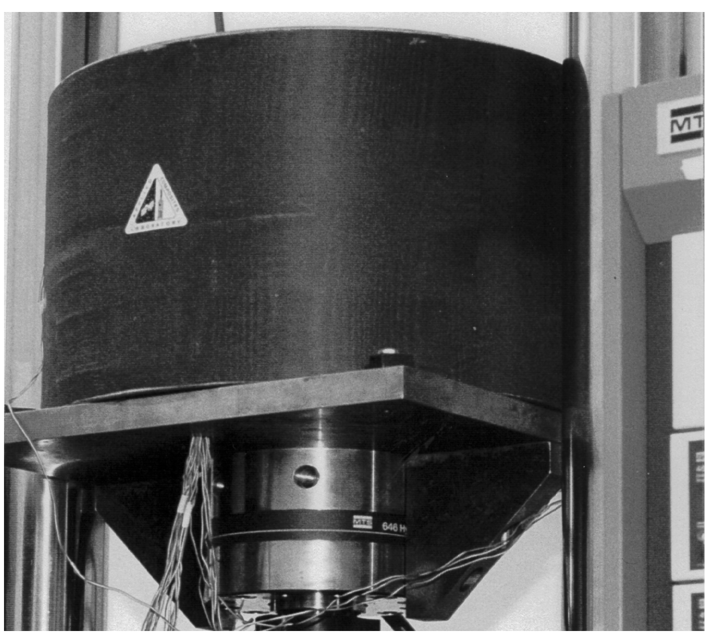

Figure 5. Compression test setup.

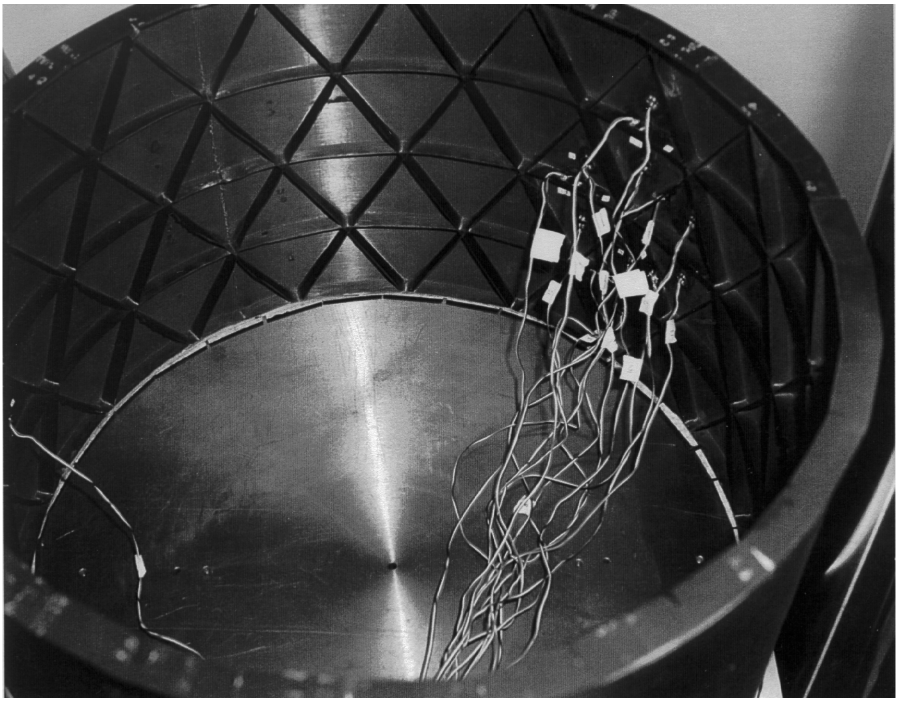

Figure 6. Location of the strain gauges.

cylinder was loaded in compression at a rate of 0.50 mm/min. The displacement controlled MTS load was continuously applied until the cylinder experienced skin buckling, and failure of stiffeners near the top and bottom edges of the cylinder occurred. The test specimen was instrumented with twenty-two strain gauges type CEA-06-125UW-350 supplied by Micro-Measurements as shown in Fig. 6. Among the strain gauges, four were uni-directional back-to-back gauges used to measure the axial and bending strains on the stiffener and skin. For the post-buckling test, twenty-two of the previous strain gauges were used. However, some of the strain gauges were damaged from the previous test run and an accurate strain data reading was not expected. Data from all strain gauges and the 80 kip bi-axial MTS test machine were recorded using a BAF-8 signal conditioner bridge and Macintosh computer. Labview and Excel software were used to obtain and plot the results.

5. TEST RESULTS

The load *versus* strain results from the original (test #1) and the post-buckling test were plotted in Figs 8 and 9. In test #1, the compression data showed that at around 40.0 kN, there was a sudden drop of a compressive load. This drop corresponded to the strain gauge values of both stiffeners and skin, which were deviating from each other. This nonlinear curve indicates the incipient buckling occurring on the

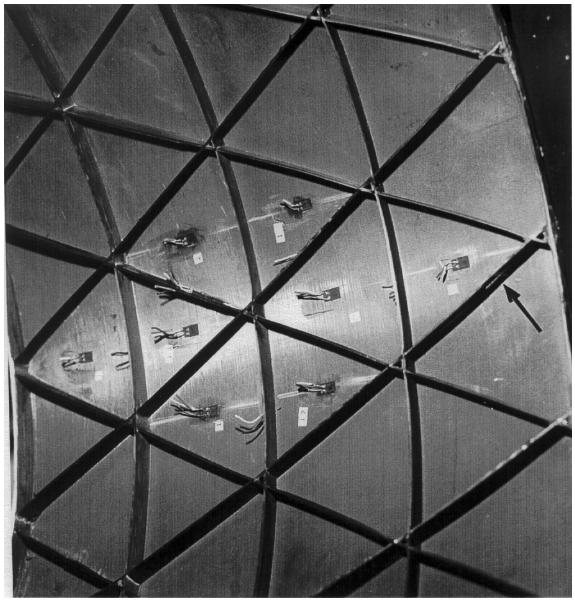

Figure 7. Location of damaged stiffener.

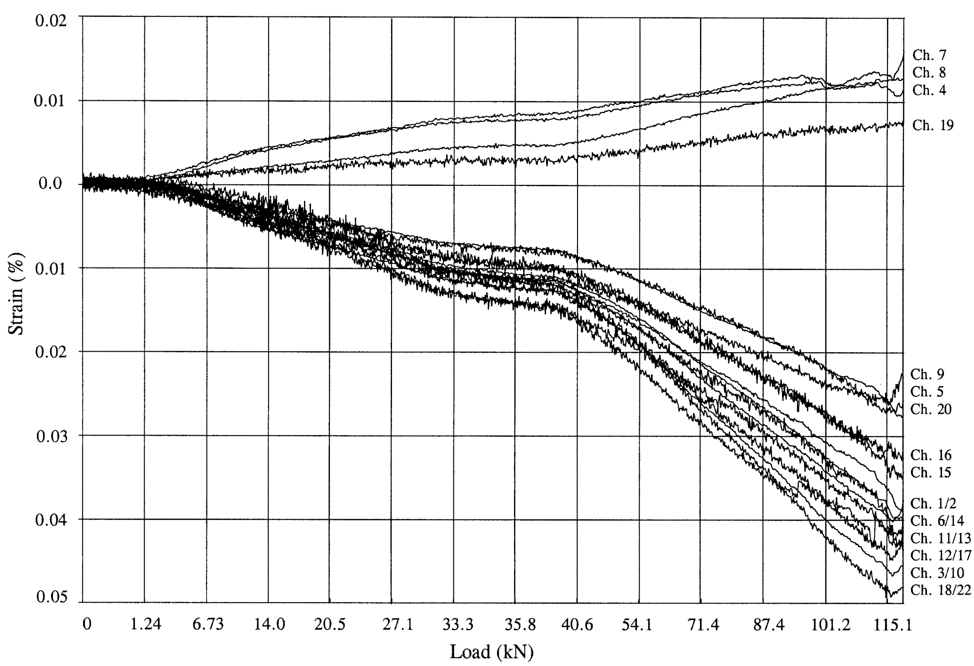

Figure 8. Load vs. strain results of test #1.

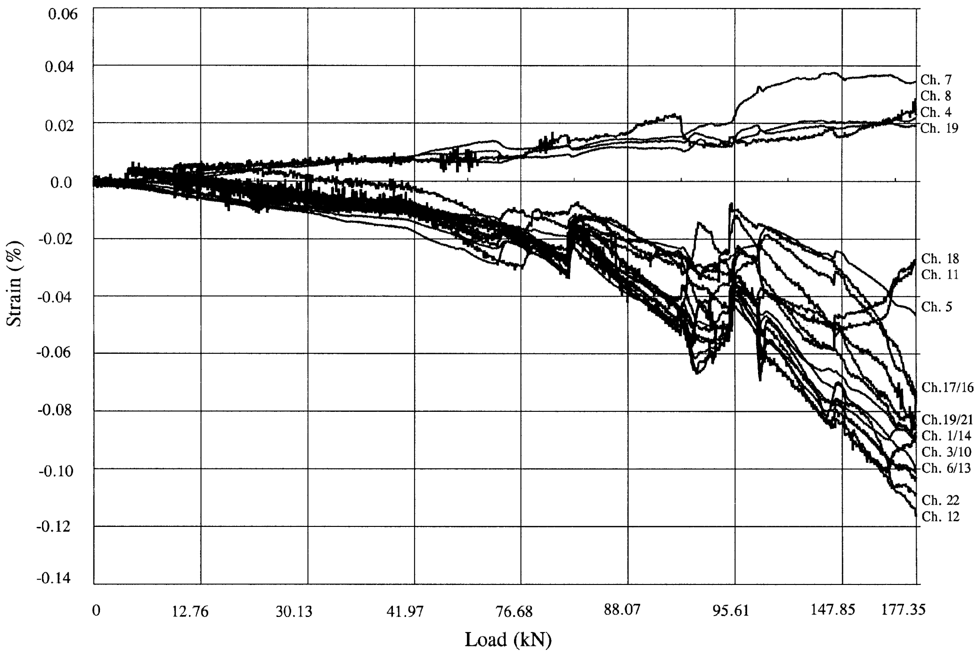

Figure 9. Load vs strain from post buckling test.

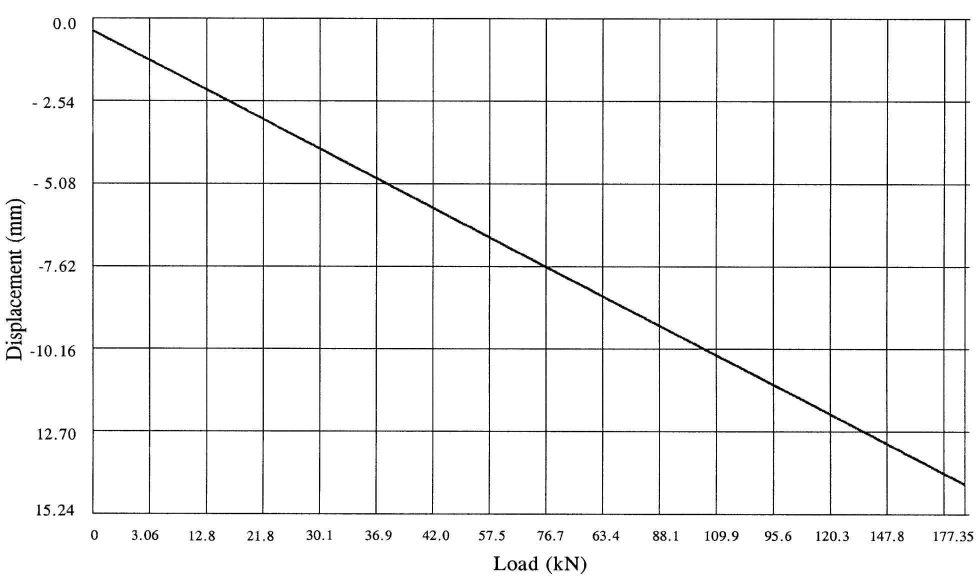

Figure 10. Load vs. displacement from post buckling test.

structure. For example, the skin strain gauges #1, #3, and #9 located on the middle of the triangular pocket area had about 10% strain difference when compared with each other. Similarly, the stiffener strain gauges #5 and #6 also began to deviate from a straight line. As the axial load reached 60.0 kN, the cylinder began to make low pinging noises caused by the polymeric matrix microcracking. The soft pinging noise was followed by a high audible cracking sound at 75 kN and another loud popping sound was heard at 106.75 kN. The test was stopped when the compression load reached 117.9 kN due to significant audible popping noises. The maximum displacement of 7.21 mm was obtained. Visual inspection of the stiffeners revealed two helical stiffeners were indeed separated from the skin located near top and bottom of the cylinder. Only one helical stiffener located near the bottom of the cylinder had a serious fracture damage. A high bending stress most likely caused this damage. However, there was no noticeable damage from the hoop stiffeners. The highest compressive strain value of 4.8% was recorded by the strain gauge #22, and the highest tensile strain value of 1.3% was recorded by strain gauge #7. The testing revealed that both stiffener and skin experience relatively large axial displacement rather than bending displacement.

The test #1 had verified that isogrid stiffeners provided most of the bending stiffness. Therefore, any damage to the stiffeners should result in the reduced buckling resistance of the cylinder. As expected during the post-buckling test, the cylinder exhibited similar buckling behavior as the previous cylinder test up to 82 kN. The helical stiffeners remained in compression and the hoop stiffeners and skin were under tension. At 63 kN, there was a sudden drop in strain followed by a distinctive loud cracking noise at 75 kN and 98 kN respectively. As the load was continuously applied, another sharp drop in strain (load relief) was encountered at 115 kN (for test #1, the testing was halted at 117 kN). The strain readings fluctuated throughout the test; eventually, the testing was stopped at 177.4 kN. Post-testing visual examination of the cylinder revealed that the upper and lower part of the cylinder (first column) showed extensive damage. As the stiffeners were no longer able to carry the load in this region, the damage intensified. The stiffeners relieved the load by transmitting it to the next set of stiffeners located in the second column before their failure. The maximum displacement of 13.75 mm was obtained as shown in Fig. 10.

Strain gauges located near the center of the cylinder had lower strain values when compared to that of strain gauges located near the top and bottom of the cylinder. The hoop stiffener resists the tendency for the helical stiffeners to bow in or out and holds the helical stiffeners stationary. This continues until one of the helical stiffeners can no longer resist high bending moment and fractures. This suggests that the load is being carried by the stiffeners and is transferred to the skin. The skin, being relatively thin, does not keep the stiffeners from local buckling. Adding additional skin layer in the circumferential direction will increase the axial stiffness, which will restrict the axial displacement in the skin. However, adding additional skin will increase the weight of the structure, which will make the structure less efficient. A better method of increasing the axial stiffness without increasing significant weight is by adding an extra hoop stiffener at the buckling node points. This extra hoop stiffener will shorten the column length, which will delay the general instability and the concentrated load will be more easily distributed into the structure. The helical stiffeners can increase their column buckling stress by utilizing the shorter end restraints provided by the hoop stiffeners. The inspection of the post-buckled cylinder revealed that four helical stiffeners had an actual fracture and another four had separated from the skin near the top and bottom of the cylinder. However, two of the four stiffeners were damaged from a previous test and all of the stiffeners located near the center of the cylinder still did not show any sign of damage, as shown in Fig. 7. The degradation of buckling resistance was low until a certain progressive damage level was reached. Even if one or more stiffeners were separated from the skin, the damaged stiffener was able to redistribute the load path to carry additional loads.

6. CONCLUSIONS

An axial compression test of a post-buckled composite isogrid structure exhibited damage tolerance and buckle resistant characteristics due to multiplicity of loading paths. The post-buckling test of the damaged cylinder exhibited similar buckling behavior as the undamaged cylinder up to 82 kN. The degradation of buckling resistance was gradual until a certain progressive damage level was reached. The compression test verified that the stiffeners are buckling critical and provided most of the bending stiffness. The stiffeners could not resist the excessive bending force and lead to the eventual failure. Even when one or more stiffeners were separated from the skin, the damaged stiffener was able to redistribute the load path to carry additional loads. The skin resisted radial displacements and increased the axial stiffness of the cylinder. Although the skin acted with stiffeners in resisting the initial bending and axial load, the cylinder's thin skin eventually could not support the stiffeners from local buckling. The post-buckled cylinder continued to resist compression loading after one or more of the stiffeners had fractured. Continued loading caused the number of fractured stiffeners to increase but the cylinder was able to maintain its basic cylindrical shape. These factors make composite isogrid cylinder attractive for use in lightweight critical structural applications.

REFERENCES

1. A. Reddy, R. Valisetty and L. Rehfield, Continuous filament wound concepts for aircraft fuselage structures, *J. Aircraft* **22**, 249–255 (1985).
2. L. Rehfield and A. Reddy, Damage tolerance of continuous filament composite isogrid structure: a preliminary assessment, in: *Composite Materials: Mechanics, Mechanical Properties and Fabrication*, Japan–US Conference, Tokyo, pp. 471–477 (1981).
3. T. Kim and C. Rotz, Warping of flat composite isogrid panels, in: *1997 IEEE Aerospace Conference*, Aspen, pp. 271–277 (1997).
4. T. Kim, Investigation of composite isogrid stiffened structures, Phillips Laboratory Technical Report 95-1112, pp. 11–21 (1995).

5. P. Seide, A Donnell-type theory for asymmetrical bending and buckling of thin conical shells, *J. Applied Mechanics* **24**, 547–552 (1957).
6. L. Li, The stability of composite material stiffened conical shell under axial compression, *Composite Structure* **38**, 169–175 (1997).
7. T. Kim, Fabrication and testing of composite isogrid stiffened cylinder, *Composite Structure* **45**, 1–6 (1999).